Insulation of the Conduction Pathway of Muscle Transverse Tubule Calcium Channels from the Surface Charge of Bilayer Phospholipid

ROBERTO CORONADO and HUBERT AFFOLTER

From the Department of Pharmacology, School of Medicine, University of North Carolina at Chapel Hill, Chapel Hill, North Carolina 27514

ABSTRACT Functional calcium channels present in purified skeletal muscle transverse tubules were inserted into planar phospholipid bilayers composed of the neutral lipid phosphatidylethanolamine (PE), the negatively charged lipid phosphatidylserine (PS), and mixtures of both. The lengthening of the mean open time and stabilization of single channel fluctuations under constant holding potentials was accomplished by the use of the agonist Bay K8644. It was found that the barium current carried through the channel saturates as a function of the $BaCl_2$ concentration at a maximum current of 0.6 pA (at a holding potential of 0 mV) and a half-saturation value of 40 mM. Under saturation, the slope conductance of the channel is 20 pS at voltages more negative than −50 mV and 13 pS at a holding potential of 0 mV. At barium concentrations above and below the half-saturation point, the open channel currents were independent of the bilayer mole fraction of PS from $X_{PS} = 0$ (pure PE) to $X_{PS} = 1.0$ (pure PS). It is shown that in the absence of barium, the calcium channel transports sodium or potassium ions ($P_{Na}/P_K = 1.4$) at saturating rates higher than those for barium alone. The sodium conductance in pure PE bilayers saturates as a function of NaCl concentration, following a curve that can be described as a rectangular hyperbola with a half-saturation value of 200 mM and a maximum conductance of 68 pS (slope conductance at a holding potential of 0 mV). In pure PS bilayers, the sodium conductance is about twice that measured in PE at concentrations below 100 mM NaCl. The maximum channel conductance at high ionic strength is unaffected by the lipid charge. This effect at low ionic strength was analyzed according to J. Bell and C. Miller (1984. *Biophysical Journal.* 45:279–287) and interpreted as if the conduction pathway of the calcium channel were separated from the bilayer lipid by ~20 Å. This distance thereby effectively insulates the ion entry to the channel from the bulk of the bilayer lipid surface charge. Current vs. voltage curves measured in NaCl in pure PE and pure PS show that similarly small surface charge effects are

Address reprint requests to Dr. R. Coronado, Dept. of Physiology and Molecular Biophysics, Baylor College of Medicine, Houston, TX 77030. Dr. Affolter's present address is Dept. of Physiology, Yale University School of Medicine, New Haven, CT 06510.

J. GEN. PHYSIOL. © The Rockefeller University Press · 0022-1295/86/06/0933/21 $1.00

Volume 87 June 1986 933–953

present in both inward and outward currents. This suggests that the same conduction insulation is present at both ends of the calcium channel.

INTRODUCTION

The electrical behavior of ion channels can be modulated by the bilayer phospholipid composition in various ways. The most direct and physically testable way is through interactions with the bilayer lipid surface charge. Studies of the effect of surface charge on channels all follow the original interpretation given by Frankenhaeuser and Hodgkin (1957) to the shifts induced by external calcium ions on the activation curve of the sodium channel. More recent work in nerve and neuron sodium, potassium, and calcium channels has shown that surface charge effects can be conveniently interpreted within the framework provided by the Gouy-Chapman theory of an electrified interphase (Gilbert and Ehrenstein, 1969; Mozhayeva and Naumov, 1970; Begenisich, 1975; Hille et al., 1975; Fohlmeister and Adelman, 1982; Kostyuk et al., 1982; Hahin and Campbell, 1983; Wilson et al., 1983; Cota and Stefani, 1984; Byerly et al., 1985).

In molluscan neurons (Kostyuk et al., 1982) and tunicate eggs (Ohmori and Yoshii, 1977), calcium and sodium channel activation curves are shifted by external divalents to the same extent. This suggests a common effect of surface potential on both channels. The numbers for the charge densities near the calcium channel "gates" range from one electronic charge per 100–240 $Å^2$, which is about the same as for sodium channels and for the composition of charged lipids in plasma membranes. However, the question of how the effect of surface charge contributes to calcium channel conduction is more complex, and this issue has not been resolved (Byerly et al., 1985). Studies in whole cells are severely limited because the only variable on hand, the ionic strength of divalent solutions, simultaneously affects (*a*) the surface potential, (*b*) the single channel current, and (*c*) the reversal potential. Thus, conduction measurements in calcium channels have multiple interpretations. For example, the saturation of calcium current with increasing external calcium has received a dual interpretation as either (*a*) a direct demonstration that surface potentials dominate ion conduction in calcium channels, since the saturation of the divalent ion concentration at the surface of a charged membrane is predicted by the Gouy-Chapman theory (Ohmori and Yoshii, 1977; Wilson et al., 1983; Cota and Stefani, 1984), or (*b*) a demonstration of a saturable binding site(s) for conducting ions inside the calcium channel (Kostyuk et al., 1974; Hagiwara, 1975; Akaike et al., 1978; see also Hess and Tsien, 1984; Almers and McCleskey, 1984).

This paper evaluates in detail the contribution of surface charge to ion conduction in calcium channels of skeletal muscle using planar bilayer techniques (Affolter and Coronado, 1985*a–c*; Coronado and Affolter, 1985*a*, *b*). Since in planar bilayer experiments the phospholipid composition can be manipulated, an effect of surface charge (or the lack of an effect) can be unambiguously demonstrated. This was done here by imposing on the channel various mole fractions of the negatively charged lipid phosphatidylserine (PS). Similarly, we evaluated the contribution of local fixed charges present in the channel itself in planar bilayers in which the bulk lipid is composed of the neutral zwitterionic lipid phosphatidylethanolamine (PE). We found that the saturation of single

channel currents with increasing bulk barium concentrations cannot be explained by the phospholipid surface charge since the current amplitudes are independent of the mole fraction of PS in the planar membrane. Small differences in the channel current amplitudes found in pure PS bilayers when compared with measurements in pure PE were revealed only after recording the sodium current through the channel in the absence of barium. The results indicate that the conduction pathway is not sensitive to the surface potential arising from the bilayer phospholipid. One possible explanation that fits the data assumes that the calcium channel conduction pathway is physically separated or insulated from the bulk lipid surface by a distance of ~20 Å.

MATERIALS AND METHODS

Muscle Membranes

Transverse tubules (t-tubules) from rat back and leg muscle were fractionated and purified according to the procedure of Rosemblatt et al. (1981) with slight modifications. Briefly, homogenization was carried out in 0.25 M sucrose (ultra-pure reagent, Bethesda Research Laboratories, Inc., Gaithersburg, MD), 20 mM histidine-Tris pH 7.4, and 0.4 mM phenylmethylsulfonylfluoride (Sigma Chemical Co., St. Louis, MO). The light microsomal fraction (surface membrane [SM]), without the Ca^{++} phosphate loading step, was used in all experiments. Vesicles were stored at −80°C in 0.5 M sucrose, 10 mM HEPES-Tris, pH 7.2, at a protein concentration of 10–20 mg/ml.

Bilayers and Lipids

Experiments were carried out in Mueller-Rudin bilayers formed from 50 mg/ml lipid solutions in decane (Aldrich Chemical Co., Milwaukee, WI). Membranes were painted in Lexan partitions with apertures of 300 μm. Bilayer capacitances were in the range 200–300 pF. Lipids were purchased from Avanti Polar Lipids (Birmingham, AL) and used without further purification. Lipids were stored at all times in chloroform at −80°C. The PE and PS (Avanti Polar Lipid catalog nos. 840022 and 850032, respectively) used in all experiments correspond to natural lipid purified from brain. The standard protocol for recording channels was as follows. Bilayers were formed in *cis* and *trans* (virtual ground side) symmetrical solutions of 50 mM NaCl, 10 mM HEPES-Tris, pH 7.0, 0.1 mM EDTA; after thinning, 100 mM $BaCl_2$ plus 1–5 μM Bay K8644 was added to the *cis* side under constant stirring and later 50–100 μg of vesicular t-tubule protein was added to the same solution. The holding potential (HP) was maintained constant at 0 mV until single channel fluctuations emerged on the record, usually within 15 min. The insertion of channels was aided in some cases by vigorous stirring and in others by the breakdown and reformation of the bilayer in the presence of t-tubule protein. Channels insert into the planar bilayer with the cytoplasmic end on the *cis* chamber and the extracellular end on the *trans* chamber (Affolter and Coronado, 1985*c*). We have found that t-tubules added to the *cis* side fuse readily in high-*cis* barium. Thus, in most experiments (but not in Figs. 3 and 6*C*), barium current was measured as flowing outward through the channel. The molar ratios of PE and PS given in the figure legends correspond to those of the lipid-decane solutions used to form bilayers.

Solutions and Activity Coefficients

In planar bilayer experiments, monovalent salts were reagent grade (Fisher Scientific, Fair Lawn, NJ) and divalent salts were analytical grade (JMC, Hertfordshire, England). Solutions were prepared from solid salts using all-glass twice-distilled water. Unless

otherwise specified, solutions were buffered with 0.1 mM EDTA, 10 mM HEPES-Tris, pH 7.0–7.4. The mean activity coefficients for $BaCl_2$ in the range 0.01–0.1 molal were obtained from the best-fitted curve of the values given by Harned and Owen (1950, Table 13-1-1). The mean activity coefficients for $BaCl_2$ solutions were as follows: 0.01 M, 0.723; 0.02 M, 0.655; 0.03 M, 0.605; 0.04 M, 0.570; 0.05 M, 0.559; 0.06 M, 0.525; 0.07 M, 0.505; 0.08 M, 0.500; 0.09 M, 0.495; 0.10 M, 0.492. The values are the molal concentration followed by the 25°C mean activity coefficient at that concentration. Single-ion activity coefficients for Ba^{++} were obtained by taking the square of the mean activity coefficient for $BaCl_2$ (Butler, 1968). Activity coefficients were used without correction for the temperature of the experiments, which was 21–22°C. The sodium activity was calculated using mean activity coefficients for NaCl; the latter were obtained from standard tables.

Handling of Single Channel Data

Records filtered at 0.05–0.1 kHz (−3-dB point from an eight-pole Bessel filter) were taken on-line and digitized at 0.5–2.0 points/ms. Records were fed into an IBM PC computer with the baseline current at a lower value than the unitary open current. The mean duration and amplitude of open events were defined using computer programs with two threshold detectors placed between the baseline and open peak current. One detector, discr 1, was placed at 1 standard deviation (SD) above the mean of the baseline current (1 SD_b); the second detector, discr 2, was placed at 1 SD below the mean of the single channel unitary current (1 SD_u). Open events are defined as transitions starting from below discr 1 that cross discr 1 and discr 2 and remain above discr 2 for two or more consecutive points. The mean amplitude of a threshold-defined open event corresponds to the arithmetic mean of all points above discr 2 minus the mean amplitude of the baseline. The filter and threshold settings given above were chosen to prevent high levels of noise spikes from crossing discr 2 and generating false events. The following considerations were made. The filter setting was selected after inspection of the degree of overlap between the unitary current and baseline current distributions on a given record. The unitary current peak and baseline current peak were fitted to a Gaussian curve to determine the standard deviations of the mean baseline current, SD_b, and unitary current, SD_u. Typical values encountered were $SD_b = SD_u = 0.06$–0.1 pA. An optimal filter setting was considered one in which the mean of the unitary current peak was 4 SD_b away from the mean of the baseline current peak. Within the noise levels of our records, this condition was satisfied by filtering at corner frequencies of 0.05–0.1 kHz in all experiments. The location of discr 1 (the threshold that initiates the count of an open transition) at 1 SD_u was roughly coincident, in most cases, with the 3 SD_b point above the baseline. From this equivalence, it is possible to calculate the rate at which noise spikes cross discr 2 and are captured as an "event." The rate of false events, λ_f, can be evaluated according to $\lambda_f = kf_c\exp(-\phi^2/2\sigma_n^2)$, where ϕ is the threshold setting measured as a distance from the baseline; σ_n is the rms baseline noise; f_c is the corner frequency; and k is a parameter that depends on the filter and baseline noise characteristics and was taken as $k = 1$ (see Colquhoun and Sigworth, 1983). With our typical noise rms value of 0.07 pA at 0.1 kHz, the maximum expected rate of false events is $\lambda_f = 0.0025\ s^{-1}$. Considering that long open events occurred at rates of $\sim 0.1\ s^{-1}$, the highest figure for the ratio of capture of a false event to a true event is 0.025. Mean amplitudes were sorted into 256 bins (0.0195–0.0039 pA/bin) and fitted to a Gaussian distribution. Curve-fitting was aided by a standard run test and by choosing parameters that minimized the sum of the squared deviations. All single points and bars in current amplitude vs. voltage, current amplitude vs. PS mole fraction, and conductance vs. activity curves correspond to the mean and SD of the

Gaussian-fitted population of open events. The number of individual open events used in these fittings was in the range of 400–1,500.

Calibration of Surface Charge Density of Bare Bilayers

The bulk negative surface charge of bilayers formed from a lipid solution containing a given mole fraction of PS was determined by the nonactin carrier conductance method of McLaughlin et al. (1971). The surface potential, $\psi(0)$, is obtained from the cationic conductance of the ion carrier nonactin measured before, $G_{[K^+]}$, and after, $G_{[K^+,Ba^{++}]}$, addition of $BaCl_2$ to both bulk solutions:

$$G_{[K^+]}/G_{[K^+,Ba^{++}]} = \exp -[\psi(0)F/RT], \tag{1}$$

where $RT/F = 25.3$ mV. Bilayers were formed from lipid solutions containing the mole fraction of negatively charged PS under test, in symmetrical 0.1 M KCl, 10 mM HEPES-Tris, pH 7.2. Nonactin was added with stirring in both chambers until the conductance stabilized at 10^{-5}–10^{-4} S/cm^2. $BaCl_2$ was then added to both sides in the concentration range 10^{-6}–10^{-1} M and conductance measurements were made after each addition. Conductance curves were normalized by plotting $\Delta \log G$ vs. log[divalent], where

$$\Delta \log G = \log G_{[K^+]} - \log G_{[K^+,Ba^{++}]}. \tag{2}$$

Eq. 2 corresponds to the decimal log form of the left-hand side of Eq. 1. The nonactin conductance described by Eq. 2 was fitted with surface potential curves derived from the Grahame equation for the case in which monovalent and divalent electrolytes are present in the bulk solution according to (McLaughlin et al., 1971):

$$\sigma = 2\epsilon\epsilon_o RT\Sigma_i C_i\{[\exp - z_i F\psi(0)/RT] - 1\}^{1/2}, \tag{3}$$

where σ is the surface charge density in electronic charges per Å^2; σ was corrected for barium-PS binding (McLaughlin et al., 1981) using an association constant of 12 M^{-1}; ϵ and ϵ_o are the dielectric constant and the permitivity of free space; C_i is the concentration of the ith species in bulk solution in moles per liter; and z_i is the valence of the ith ion. The surface charge density of bilayers containing a test mole fraction of PS was estimated by superimposing the nonactin conductance data on Grahame curves in which $\psi(0)$ appears in a dimensionless form, $\Delta\psi(0)$:

$$\Delta\psi(0) = \psi(0)^{max}F/2.3RT - \psi(0)F/2.3RT, \tag{4}$$

where $\psi(0)^{max}$ is the surface potential in the limit of zero divalent, and $\psi(0)$ is the surface potential at a given divalent concentration. Eq. 4 corresponds to the decimal log form of the right-hand side of Eq. 1. In our hands, the nonactin conductance method yielded a surface charge density of 1 electronic charge per 2,000 Å^2 for 100% PE and 1 charge per 50 Å^2 for 100% PS at pH 7.0 (Table I). At face value, these determinations are assumed to be correct since they agree with the results of Bell and Miller (1984) and the original results of McLaughlin et al. (1971). The calibrated data of the mole fraction PS in the planar bilayer vs. the mole fraction of PS in the lipid-decane painting solution are given in Table I.

Calculation of Sodium Concentration Near the Membrane Surface

The concentration of monovalent electrolyte at a given distance from the membrane surface was calculated after solving $\psi(x)$, the electrostatic potential at a distance, x, with a knowledge of the surface potential and the surface charge density as described by Bell and Miller (1984):

$$\psi(x) = [2RT/F] \ln\{[1 + \alpha \exp(-Dx)]/[1 - \alpha \exp(-Dx)]\}; \tag{5a}$$

TABLE I

Calibration of Surface Charge Density

Lipid	Surface charge density	Mole fraction, X_{PS}
	charges/100 Å²	
PE, pH 7.0	0.05 (0.04 SD)	0.025 (0.034)
PS, pH 7.0	2.0 (0.3 SD)	1.000 (1.400)
2:1 PE/PS pH 7.0	0.1 (0.1 SD)	0.075 (0.070)
1:1 PE/PS pH 7.0	0.3 (0.12 SD)	0.175 (0.210)
1:2 PE/PS pH 7.0	0.75 (0.13 SD)	0.40 (0.520)

Charge density was calculated with the nonactin K^+ method using Eqs. 1–4. $X_{PS} = 1.0$ was taken as the charge density obtained in 100% PS. The mole fractions estimated from the measured charge density assuming a molecular area of 70 Å² per phospholipid are given in parentheses (Loosely-Millman et al., 1982).

$$\alpha = \{\exp[F\psi(0)/2RT] - 1\}/\{\exp[F\psi(0)/2RT] + 1\}, \quad (5b)$$

where $D = [2F^2Na^+(b)/\epsilon\epsilon_o RT)]^{1/2}$ is the reciprocal of the Debye length, which varies with the bulk sodium concentration, $Na^+(b)$. $Na^+(x)$, the concentration of Na^+ at a distance x, is calculated from a Boltzmann distribution in the electrostatic potential:

$$Na^+(x) = Na^+(b)\exp[-F\psi(x)/RT]. \quad (6)$$

The surface potential, $\psi(0)$, in Eq. 5*b* was calculated from the measured surface charge density and the bulk sodium activity, as in Eq. 3. $Na^+(x)$ was calculated from Eq. 6 after solving $\psi(x)$ (Eqs. 3, 5*a*, and 5*b*) by an iterative procedure.

RESULTS

Amplitude Distributions of Barium Currents

Fig. 1 shows barium current through single Bay K8644–activated calcium channels inserted into lipid bilayers composed of pure PE, pure PS, and a 1:1 mixture

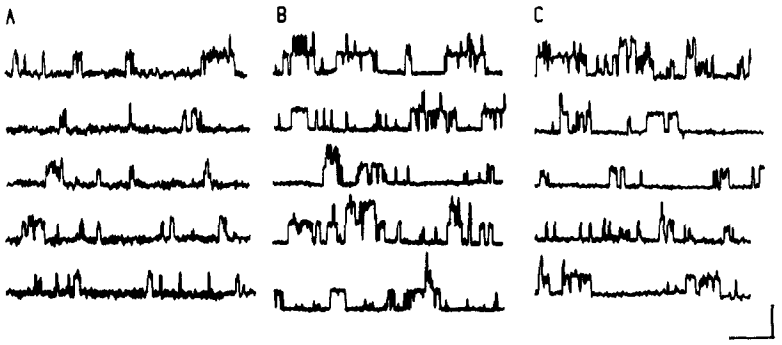

FIGURE 1. Barium current through t-tubule calcium channels inserted in neutral and negatively charged planar bilayers. Records at HP = 0 mV of barium current in bilayers formed from pure PE (*A*), a 1:1 mixture of PE/PS (*B*), or pure PS (C). *cis* 0.05 M NaCl, 0.1 M $BaCl_2$; *trans* 0.05 M NaCl. Calibration bars for all records are 0.8 pA (vertical), 800 ms (horizontal).

of both (mole fraction in bilayer-forming solution). The channel amplitudes in all lipid mixtures were found to be remarkably similar. However, there are considerable differences in kinetics since the openings in PE are ~30% shorter than those in PS or PE/PS (1:1) (not shown). The traces shown are noncontiguous and representative of the quality of data collected for analysis. The use of Bay K8644 in the present work serves two purposes. First, the agonist permits a pharmacological separation of the barium (or sodium) current carried through calcium channels from the agonist-insensitive residual barium (or sodium) current, which could in principle be carried by other channels present in the same preparation (see Coronado and Affolter, 1985*b*). Second, the use of the agonist solves in part the inherent bandwidth limitations associated with recordings in large planar bilayers, inasmuch as 35% of Bay K8644–induced events have a lifetime longer than 150 ms (Affolter and Coronado, 1985*b*). Fig. 2 (left panel)

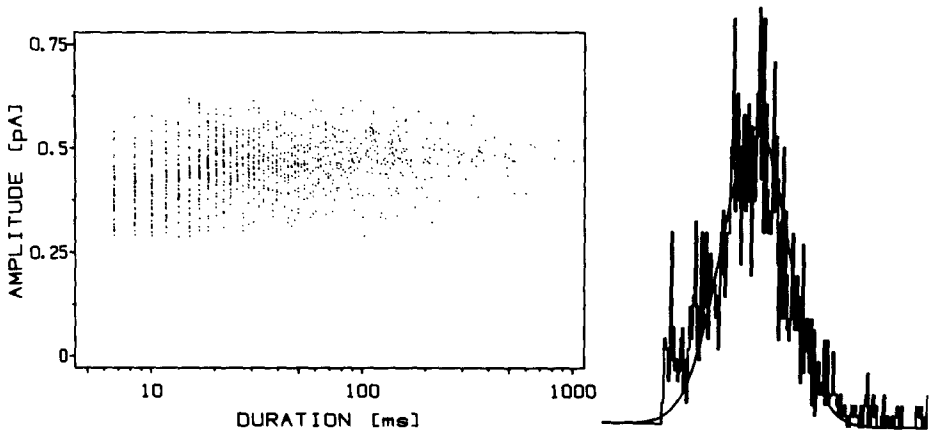

FIGURE 2. Duration-amplitude characteristics of unitary barium currents. Left panel: mean amplitude and mean duration of 855 openings at HP = 0 mV, a 1:1 mixture of PE/PS in *cis* 40 mM $BaCl_2$. Each opening is a single point. Right panel: 1,155 events (as above) are plotted as occurrences (*y*-axis) vs. current amplitude (*x*-axis). Events shorter than 20 ms are not included. The smooth curve corresponds to a Gaussian fit with a peak amplitude of 0.44 pA and a standard deviation (SD) of 0.07 pA.

shows openings plotted as amplitude (*y*-axis) vs. duration (*x*-axis). Each point in this plot is a single event collected using the filter settings and threshold crossing points described in Materials and Methods. After calculation of the mean amplitude at each duration, it was possible to set a cutoff that would eliminate the unresolved short openings without a loss of large numbers of nonattenuated samples. This cutoff was arbitrarily set at 20 ms because events at 20 ms always had the same mean amplitude as events of ≥100 ms. An amplitude distribution of unitary events above the 20-ms cutoff is given in the right panel of Fig. 2 for 40 mM $BaCl_2$ in PE/PS. The fitted Gaussian curve (solid line) shows that in mixed lipid conditions or pure lipid (not shown), the population of channels is described by a single unitary current level. Inasmuch as the samples above and below the mean are roughly even, the 20-ms cutoff appears to be satisfactory.

Sublevel currents, lower than the unitary current, have been observed in ~1 of every 50 openings. In the present analysis, the subunitary events were rejected when they were present below the threshold detectors. Those slightly above threshold generated in some cases a shoulder in the amplitude distribution (see Fig. 2, right panel).

Fig. 3 shows the current-voltage curve for the channel conducting inward barium current (negative current) in the range of +100 to −100 mV. A few points of the outward barium current around HP = 0 mV (positive current) are also shown. The internal and external sides of the channel are always found in the *cis* and *trans* bilayer chambers, respectively (Affolter and Coronado, 1985*c*). The slope conductance at 0.1 M Ba^{++} is 20 pS at voltages more negative than

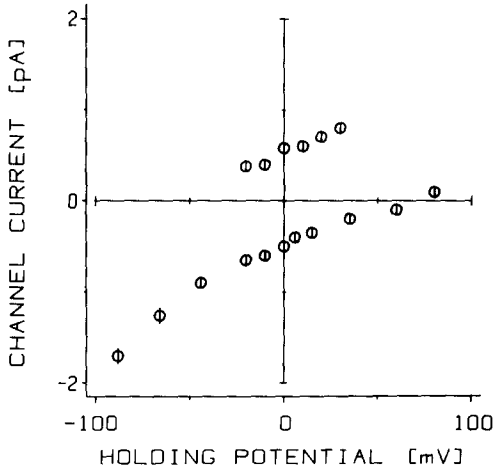

FIGURE 3. Inward and outward barium currents at saturation. Negative (inward) currents are given in *trans* (external) 0.1 M $BaCl_2$, *cis* (internal) 0.25 M NaCl. The reversal is at +61 mV. Six data points of positive (outward) current around 0 mV were measured in *trans* (external) 0.25 M NaCl, *cis* (internal) 0.1 M $BaCl_2$. Bilayers correspond to 1:1 PE:PS; bars correspond to 1 SD.

−50 mV, 13 pS at HP = 0 mV, and 8 pS close to reversal (+61 mV). This voltage dependence is probably due to the asymmetry of the solutions chosen in this experiment since the current-voltage curve is approximately linear in near-symmetrical conditions (see Fig. 9). When measured separately, under equivalent ionic conditions, the inward and outward barium currents appear to have the same amplitude and slope conductance at HP = 0 mV.

Absence of Surface Charge Effects on Barium Currents

In bilayers composed of a 1:1 mixture of PE/PS (=1 e/333 $Å^2$; see Table I), outward barium currents saturate with increasing *cis* $BaCl_2$ (Fig. 4). The maximum current at HP = 0 mV is 0.66 pA at 0.6 M, and the half-saturating $BaCl_2$ concentration is ~40 mM. The shape of the saturation curve was analyzed by plotting data in the Langmuir form, as *i* (current) vs. Ba (barium activity) (Fig.

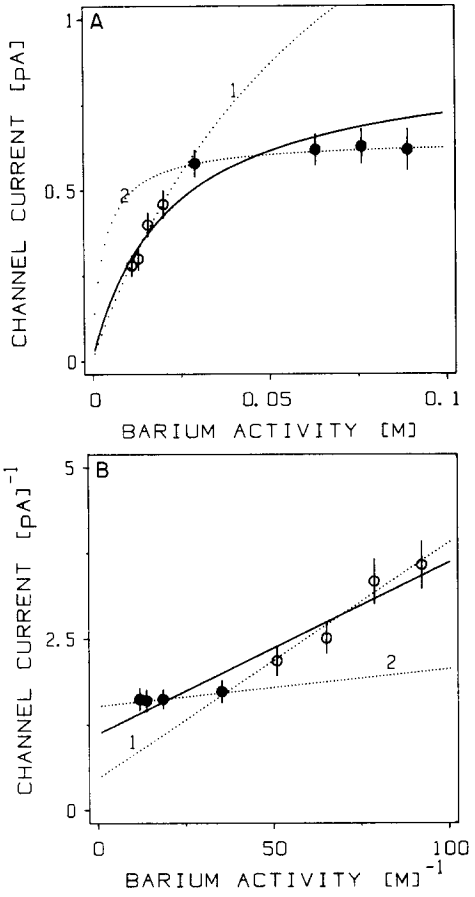

FIGURE 4. Saturation of barium current as a function of *cis* $BaCl_2$. Mean and 2 SD of currents are given at HP = 0 mV in 1:1 PE/PS. Solutions were *trans* 50 mM NaCl, *cis* 50 mM NaCl plus the indicated activity of Ba^{++} (chloride salt). Plots correspond to (*A*) i (channel current) vs. Ba (barium activity), and (*B*) $1/i$ vs. 1/Ba. Parameters of fitted curves are: solid line: i_{max} = 0.89 pA, K = 22 mM, r = 0.90; dotted line 1: i_{max} = 2.12 pA, K = 72 mM, r = 0.96; dotted line 2: i_{max} = 0.65, K = 3.5 mM, r = 0.97. K is the half-saturation constant, r is the linear regression coefficient. Dotted line 1 was fitted to the first four points (open circles) and dotted line 2 to the last four points (solid circles) of the saturation curve. The solid line was fitted to all points.

4*A*) and as $1/i$ vs. 1/Ba or in double-reciprocal Lineweaver-Burk form (Fig. 4*B*). The barium activity at each molar concentration was calculated by taking the square of the mean activity coefficient for $BaCl_2$ (see Materials and Methods). There are two observations suggesting that saturation does not follow a single Langmuir isotherm. First, the double-reciprocal data below 0.1 M (open circles) are best fit by a straight line (dotted line 1), which has parameters different from

that used to fit the data at 0.1 M and above (solid circles, dotted line 2). The solid line is a fit to the complete set of data. The saturation parameters obtained from the slope and intercept of lines 1 and 2 are given in the Langmuir plots (Fig. 4*A*) as dotted curves 1 and 2, respectively. We have found that any attempt to fit the low-concentration part of the curve leaves the high-concentration points at 5 SD or more away from the isotherm. The same happens to the low-concentration points when the high-concentration points are fit first. Thus, it appears that saturation is best described by two rather than one isotherm. Second, the least-squares line for the complete set of data gives a correlation coefficient that is lower than that of line 1 or 2 (see the legend to Fig. 4).

The contribution of negative surface charge to barium currents was examined in Fig. 5 by recording calcium channels in bilayers with known amounts of PS. Measurements were made at three bulk $BaCl_2$ activities (calculated from mean salt coefficients): that representing the saturating current (49 mM, top panel), a nonsaturating current above the half-saturation point (27 mM, middle panel), and a current below the half-saturation point (15 mM, bottom panel). The amplitudes at each barium activity are independent of the molar fraction of PS, X_{PS}. The latter was experimentally changed at the expense of the neutral lipid, PE. In each panel, the only variable is X_{PS} while barium activity and the holding potential are maintained constant. In order to keep the same signal-to-noise ratio at the three barium activities, the holding potential was adjusted to a different value in each panel. In spite of the fact that the surface potential on the divalent side is changed in all three cases by ~40 mV when X_{PS} is varied from 0 to 1 and the surface divalent concentration is raised above the bulk concentration by a Boltzman factor of 25, the measured single channel currents remain the same in all lipid mixtures. In the top panel, the two most different means have a 20% overlap in SD. In the middle and bottom panels, the overlap is ≥50%. Equally significant is the fact that the currents seem to have no consistent trend either to increase or decrease when PS or PE becomes the dominant lipid.

Sodium Current Through Calcium Channels in the Absence of Barium Ions

Sodium current can be transported through single t-tubule calcium channels under conditions of low divalent and high monovalent concentrations (Fig. 6). Previous work has shown that the monovalent current is similar to the divalent current in that it can be blocked by micromolar nitrendipine (K_i = 0.7 μM) and by D600 (K_i < 20 μM) (Coronado and Affolter, 1985*a*, *b*). Fig. 6*A* shows records of outward channel currents with NaCl-EDTA (0.1 mM) solutions as the only current carrier. Unitary currents in sodium exceed 1 pA, at concentrations in which the pure barium current (Fig. 4) or the mixed sodium-plus-barium current (Fig. 6*B*, triangles) is ≤0.5 pA. Fig. 6*B* compares side by side the amplitudes of currents carried by Na^+ (squares) or by the same molar concentrations of Na^+ and Ba^{++} added together (triangles). The mixed Na^+-Ba^{++} current saturates at ~0.5 pA, whereas the Na^+ current alone may be as high as 2 pA at 1 M *cis* (internal) NaCl. Thus, the monovalent and divalent currents transported through the channel are not additive. Fig. 6*C* shows that the sodium and barium currents display an anomalous mole fraction behavior. In this experiment, the *cis* (internal)

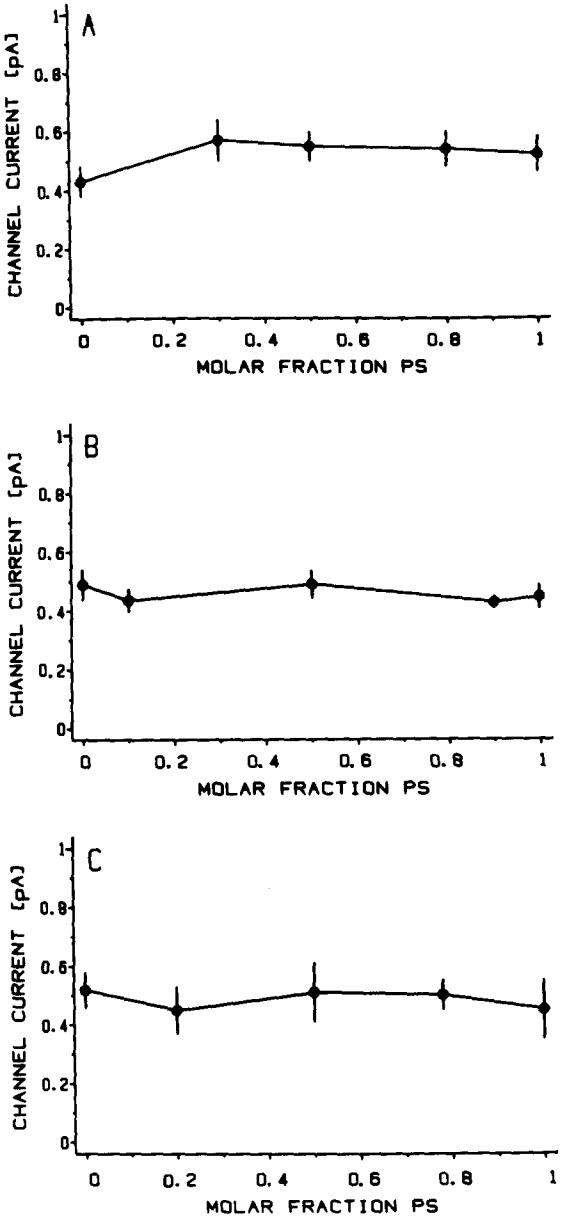

FIGURE 5. Absence of surface charge effects on Ba^{++} single channel currents. Mean current and 2 SD are given at HP = 0 mV and 49 mM barium activity (*A*), HP = +10 mV and 27 mM barium activity (*B*), and HP = +50 mV and 15 mM barium activity (*C*) (calculated from mean salt activity coefficients), and the indicated mole fraction of PS. $X_{PS} = 0$ corresponds to bilayers formed from 100% PE. The mole fraction corresponds to that present in the lipid-decane solution at the moment of forming the bilayer. The solid lines connecting means have no theoretical significance.

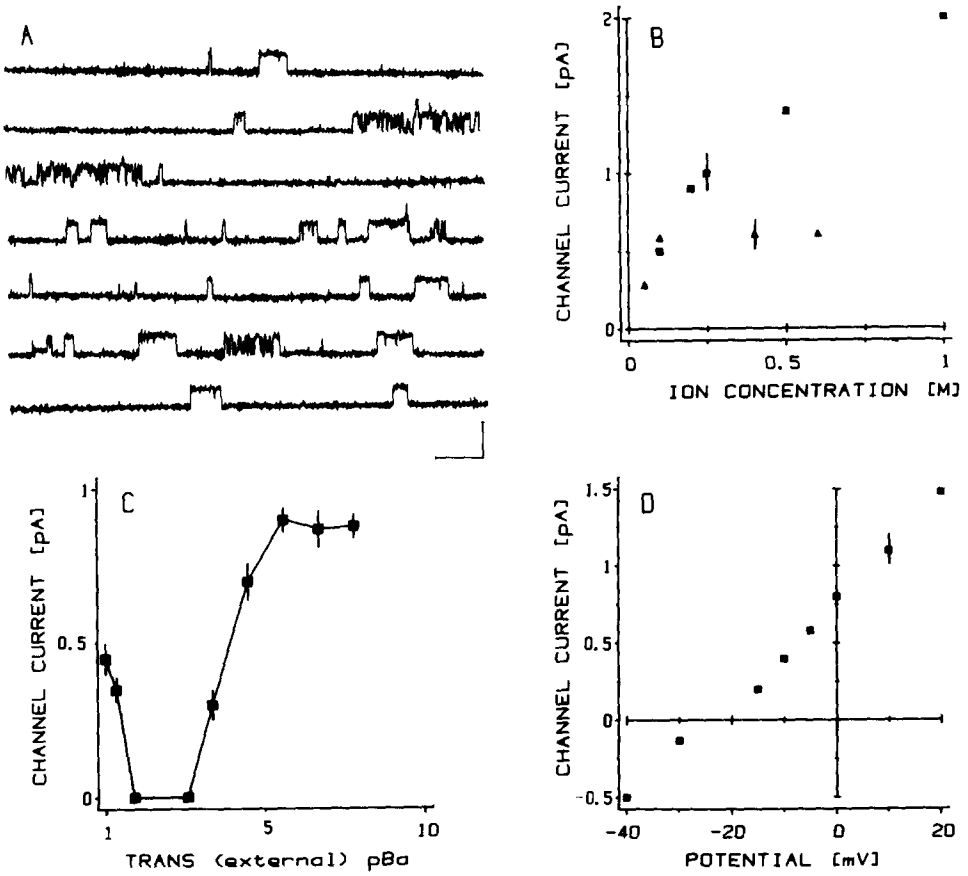

FIGURE 6. Sodium current through the t-tubule calcium channel. (*A*) Contiguous records of Na^+ current at HP = 0 mV in *trans* 0.05 M NaCl, *cis* 1 M NaCl. Calibration bars are 3 pA and 400 ms. (*B*) Amplitude of single channel currents at HP = 0 mV measured in constant *cis-trans* 0.05 M NaCl, and a variable *cis* [$BaCl_2$] given by the triangles, or in constant *trans* 0.05 M NaCl, *cis* 0.01 M $BaCl_2$, and a variable [NaCl] given by the squares. Concentrations are not corrected for ionic activities. The bars indicate the largest SD. (*C*) Effect of molar fraction of *trans* (external) Na^+-Ba^{++} solutions on current amplitudes. Currents are at HP = 0 mV in *cis* 0.25 M NaCl, *trans* 0.1 M [$BaCl_2$ + NaCl]. *trans* $BaCl_2$ was varied between 10^{-8} and 10^{-1} M, maintaining a constant [$BaCl_2$ + NaCl] of 0.1 M. (*D*) Current-voltage curve under bi-ionic Na^+-K^+ conditions containing *trans* 0.125 M KCl, *cis* 0.25 M NaCl. The reversal occurred at −22.5 mV. The single bars indicate the largest SD.

Na^+ was maintained constant at 0.25 M and the *trans* (external) molar fraction of $BaCl_2$ was varied between $X_{Ba} = 1.0$ and $X_{Ba} = 10^{-7}$ at the expense of NaCl. When $BaCl_2$ was ≤1 μM, currents were outward and the current carrier was Na^+. Chloride is impermeant, since the reversal of currents in NaCl was at E_{Na} (Fig. 9). $BaCl_2$ above 1 μM progressively reduced the amplitude of the sodium

currents, which disappear from the records at ~0.5 mM $BaCl_2$. At concentrations above 10 mM $BaCl_2$, channel currents re-emerge, but as inward currents that saturate at ~0.5 pA and have reversal potentials closer to E_{Ba} and away from E_{Na} (not shown). Thus, the sodium current measured here is transported via calcium channels. Fig. 6*D* clarifies that what we refer to as sodium current through the channel is only nominally so, given that potassium ions are almost equally permeable. The Goldman permeability ratio, P_{Na}/P_K, is 1.4. Hence, in the absence of divalent cations, the calcium channel is cation selective with low selectivity between Na^+ and K^+.

Small Surface Charge Effects on Sodium Current

The monovalent current through calcium channels was used to measure the contribution of lipid surface potential to conduction. Fig. 7 shows conductance–

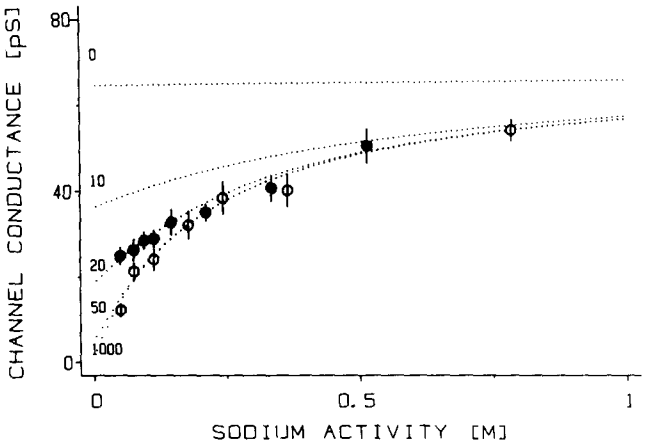

FIGURE 7. Saturation of sodium current in neutral and charged bilayers. The slope conductance was measured in the range of +10 to −10 mV in bilayers composed of 100% PE (open cirles) or 100% PS (solid circles). Solutions were symmetrical *trans* and *cis* 0.1 mM EDTA plus the NaCl activity indicated on the *x*-axis. The dotted lines were calculated from Eqs. 5*a*, 5*b*, 6, and 7 using the surface charge density of PS given in Table 1 (0.02 e/Å^2). The distances separating the entryway from the bilayer surface are indicated in angstroms next to each curve.

sodium activity relationships under symmetrical NaCl for channels inserted in pure PE or pure PS bilayers. In PE, the data are well described by a rectangular hyperbola of the form $g = g_{max}/[1 + K/Na^+(b)]$ (Eq. 7), with a maximum conductance $g_{max} = 68$ pS, and a half-saturation bulk activity $K = 0.2$ M (see the linear fit in Fig. 8). In PS, the amplitudes below 0.1 M activity were consistently higher than those in PE. At 48 mM, the PS and PE data differed by a factor of 1.8. At high ionic strength, the PE and PS data are indistinguishable. We have interpreted the differences at low ionic strength in terms of a local increase in sodium ion activity that PS may generate near the entry to the channel. The questions of whether (*a*) deviations in PS are consistent with a description of

surface charge as in the Gouy-Chapman theory, and (b) how much of the negative surface potential contributes to conduction, were answered by fitting simultaneously the conductance-activity curves in PE and PS as follows. The term corresponding to bulk sodium activity, $Na^+(b)$, in the Langmuir isotherm (Eq. 7) was replaced by $Na^+(x)$, the sodium concentration existing at a distance, x, normal to the surface of a charged membrane. The rationale here is that the ion concentration relevant to conduction is not that given by the bulk solution but by the concentration near the entryway or mouth; in this model, the mouth is separated from the lipid by distance, x. The latter can be estimated by solving $Na^+(x)$ and by using the Langmuir isotherm to describe conduction in the channel. The results of these calculations are shown in Fig. 7 and are given by

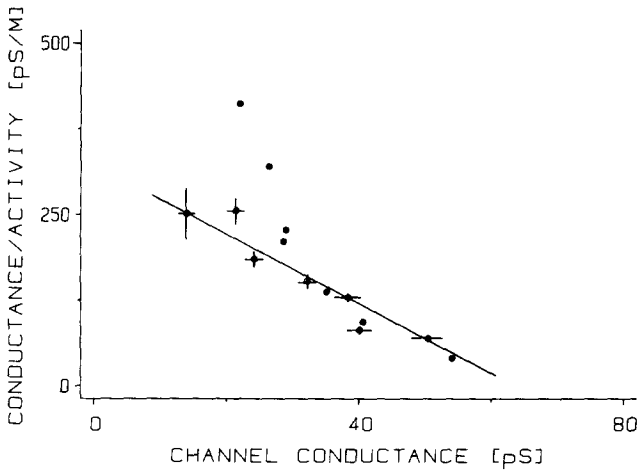

FIGURE 8. Eadie-Hofstee representation of sodium saturation. The conductance saturation in NaCl given in Fig. 7 is plotted as conductance/[NaCl] vs. conductance for PE (open circles) and PS (solid circles). The vertical and horizontal bars correspond to the SD of the PE data. The solid line was drawn with a slope $-1/K = 5\ M^{-1}$ and an x-intercept $g_{max} = 68$ pS.

the dotted lines. Each curve corresponds to a Langmuir-type saturation at a fixed distance, x, indicated in angstroms in each curve. In pure PS, the channel conductance senses less than the full surface potential given by the 0-Å curve but is well described by the curve at 20 Å. Hence, the channel is insulated from the bulk of the lipid surface charge. In pure PE, conductance may be equally well described by curves with $x = 50$ or 1,000 Å. This shows that in channels in PE there is practically no effect of surface charge. The Langmuir isotherm chosen in this analysis is justified by the Eadie-Hofstee plot in Fig. 8. In PE, this representation gives a straight line from 0.05 to 0.8 M, a concentration range that spans four half-saturation constants ($K = 0.2$ M). Thus, when no lipid charges are imposed on the channel, conductance becomes a simple function of bulk activity. By comparison, the PS data in the same plot (solid circles) bend upward at low ionic strength. Fig. 9 compares under identical conditions Na^+

current-voltage curves in PE and PS. Both the inward and outward currents appear to be largely insensitive to lipid charge. By implication, then, both ends of the channel are insulated. Curves were taken at low ionic strength in order to increase the surface potential on both sides of the bilayer and thus make the effect of PS noticeable to inward and outward currents. No differences in PE vs. PS at voltages near reversal are discernible. At 30 mV above and below reversal, measurements in PS exceed those in PE by a factor of ≤ 1.5.

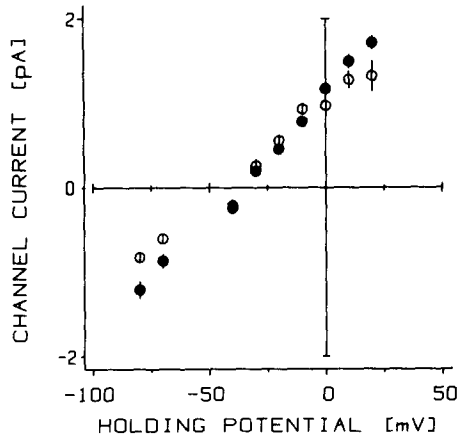

FIGURE 9. Open channel current vs. voltage curve in PE and PS bilayers. The mean and 2 SD (vertical bars) of current amplitudes in 100% PE (open circles) or 100% PS (solid circles) are given. *trans* 0.02 M NaCl, *cis* 0.08 M NaCl. The reversal was at −35.5 mV ($E_{Na} = -35$ mV).

DISCUSSION

Absence of Contribution of Phospholipid Surface Charge to Barium Conduction

Since gating characteristics of calcium channels change with surface potential, it has been assumed that the same surface potential contributes to ion conduction. This assumption has been made for practically all calcium channels, including those of skeletal muscle (Cota and Stefani, 1984). In the present work, we tested this hypothesis in a direct manner by reconstituting calcium channels in planar bilayers composed of neutral and charged phospholipids. Because the area of a planar bilayer is about five orders of magnitude larger than the average area of a single purified t-tubule vesicle (Rosemblatt et al., 1981), when a vesicle fuses to a planar bilayer, channels are effectively transferred into a vast excess of exogenous lipid. This drastically modifies the bulk lipid charge environment but leaves the ionic strength of solutions constant. Obviously, these manipulations cannot be performed in vivo. However, they are crucial for testing the contribution of lipid charge to channel conduction. The data demonstrates that barium conduction is independent of bilayer surface charge. This was shown by measuring barium unitary currents at three different activities above and below the midpoint of the conductance-activity curve (Fig. 5). The latter is important since

an absence of an effect of PS on a channel driven into saturation by high barium is less meaningful in this case. The observation that the ion entryways are probably located several Debye lengths away from the membrane surface is sufficient to explain why the effects of PS are measurable in Na^+ (Fig. 9) but not in Ba^{++} (Fig. 5). For a 100% PS bilayer bathed in 0.1 M monovalent salt. ψ (x = 20 Å), the electrostatic potential at a distance of 20 Å (Eqs. 5*a* and 5*b*) is about −12 mV and the monovalent cation concentration at that distance, C^+ (x = 20 Å), is 0.16 M (Eq. 6). The same calculation for 0.1 M divalent salt shows, however, that ψ (x = 20 Å) is approximately −2 mV (Carnie and McLaughlin, 1983) and C^{++} (x = 20 Å) is 0.117 M. The expected single channel conductance ratio in neutral and charged bilayers, g(PS)/g(PE), then becomes 1.33 for 0.1 M Na^+ but only 1.04 for 0.1 M Ba^{++}. Thus, changes in barium current of this magnitude could not be detected, since in the amplitude distributions, 1 SD was typically within 10–15% of the mean (Fig. 2). These calculations also point to fact that, in vivo, the lipid surface charge probably does not contribute to calcium channel conduction at all. Using a charge density of 0.003 e/Å^2, which corresponds to 17.5% PS (Table I) and agrees with the acidic lipid content of t-tubules (Rosemblatt et al., 1981), and a mixed monovalent-divalent solution composed of 0.1 Na^+, 0.01 M Ca^{++} (Almers and McCleskey, 1984), the surface potential calculated from the Grahame expression (Eq. 3) is −40 mV. An upper limit for ψ (x = 20 Å) can be obtained by neglecting divalents. This value is close to −5 mV; hence, neither monovalent nor divalent currents would appear to be sensitive to surface charge.

The question of charges present at the channel's mouth can be answered in some detail by the Eadie-Hofstee representation of the sodium conductance data in neutral PE membranes (Fig. 8). When the bulk of the lipid was made neutral, we expected to see conductance changes caused by surface potentials surrounding the entryways of the channel. When present, these local fields perturb the concentration profile of ions close to the ion binding site(s) involved in conduction (Apell et al., 1979). Any significant deviation from linearity in the Eadie-Hofstee representation may thus arise from electrostatic fields surrounding these sites. The plot shows, however, a strict linearity down to 40 mM NaCl. The sensitivity of this plot to weak electrostatic fields is thoroughly justified by the conductance in PS bilayers. At low ionic strength, the PS data take a noticeable upward bending in spite of the fact that the negative charges of PS are 20 Å away from the mouth of the channel. Thus, the absence of measurable deviations in pure PE argues that the sodium binding site(s) and the closest net charge in the channel's mouth are probably separated by much more than 20 Å. Based on the effective distance that is necessary to fit conductance saturation in PE, this distance is likely to be >50 Å (Fig. 7). The density of these charges would be <1 e/250 Å^2. However, since what is measured is an effective distance, the equations do not rigorously distinguish between a single charge of $z = -1$ or two charges of $z = -1/2$, etc. Hence, the density of partial charges or dipoles lining the mouths of the pore could probably be higher. If in reality the entryways had a density of 1 charge per 250 Å^2, this would probably amount to one charge or less per entryway. This is because the largest molecule that can fit into the

calcium channel has been shown to be tetramethylammonium (TMA), which has a diameter of ~6 Å (McCleskey and Almers, 1985; McCleskey et al., 1985). The smallest conceivable entryway would be a cavity that can completely surround TMA on all sides. Such an entryway would have an area of ~150 $Å^2$, which is smaller than the estimated area per charge. The symmetry of the current-voltage curve in sodium (Fig. 9), however, argues that regardless of the actual number of dipoles and partial charges at the mouths, the intracellular and extracellular ends of the channel are equally insulated.

Origin of the Sodium Current Through Calcium Channels

The observations that (*a*) the saturating conductance in Na^+ is 68 pS, whereas that in Ba^{++} at HP = 0 mV is 13 pS, (*b*) the Goldman permeability ratio favors Ba^{++} (Fig. 3), and (*c*) currents in Ba^{++} and Na^+ give rise to an anomalous mole fraction effect (Fig. 6*C*) suggest that conduction in this channel proceeds via multiple interacting sites. In vivo, this has been demonstrated for both skeletal and cardiac calcium channels (Almers and McCleskey, 1984; Hess and Tsien, 1984). Single-site, single-ion conduction can be directly ruled out in this case by evaluating the conductance affinity permeability condition for Na^+ and Ba^{++} in mixed solutions. In one-ion pores, the saturating conductance ratio for any two permeating ions (X, Y), $g(Y)/g(X)$, and the binding affinity ratio or ratio of half-saturation constants, $K(X)/K(Y)$, and the Goldman permeability ratio, $P(X)/P(Y)$, are all linked by the relation (Coronado et al., 1980):

$$g(Y)/g(X)K(X)/K(Y)P(X)/P(Y) = 1. \quad (8)$$

In this case, Eq. 8 has a low limit of 13.7–19.5, given a conductance ratio $g(\mathrm{Na})/g(\mathrm{Ba}) = 5.2$, a permeability ratio $P(\mathrm{Ba})/P(\mathrm{Na}) = 25$ (Affolter and Coronado, 1985*b*), and a binding affinity ratio $K(\mathrm{Ba})/K(\mathrm{Na}) = 0.11$ or 0.15, depending on whether single ion activity coefficients of mean salt coefficients are used (Fig. 4). This means that one ratio of variables is at least 10-fold larger or smaller than can be expected for conduction as in single-ion channels. For true single-ion channels, Eq. 8 varies between 1.0 and 1.6 for several ion pairs (Coronado et al., 1980).

The anomalous mole fraction behavior is perhaps the most convincing evidence that the bilayer channels are the same as those recorded macroscopically by Almers and McCleskey (1984) in frog skeletal muscle. This phenomenon can be explained, as done in vivo, by postulating (*a*) a tighter binding of barium over sodium inside the calcium channel, which would explain the inhibition for the sodium current by micromolar barium (Fig. 6*C*), and would ensure a high rate of sodium flow when barium is not present (Fig. 6*B*); (*b*) adherence of the channel to the laws of ion occupancy and translocation described for multi-ion single-file pores; and (*c*) ion-ion repulsion inside the pore to boost the single channel conductance. The last would explain the reappearance of current when barium is increased in the millimolar range (Fig. 6*C*). There are quantitative differences between bilayer and in vivo that should be pointed out. The half-blocking constant for Ba^{++} in Fig. 6*C* is ~100 μM, whereas the blocking constant for Ca^{++} in frog is ~1 μM. This may be related to the observation in snail calcium

channels (Kostyuk et al., 1983) that Ba^{++} block of sodium current has a 100-fold-lower affinity than Ca^{++} block.

T-Tubule Calcium Channels Are Probably Large Macromolecules

Because many different geometries of channels can generate the same answer, the physical interpretation of the insulating distances is still fuzzy. Inferred distances for several channels are given in Table II and correspond to ~10 Å for K^+ channels but ≥20 Å for Ca^{++} and Na^+ channels. The electrostatic nature of the measurement is confirmed in Table II by the dependence of the conductance ratio PS/PE on ionic strength, being much more prominent at 50 mM than at 500 mM. This appears to hold for all cases analyzed. In terms of models, insulation can be interpreted as a vertical distance (normal to the plane of the

TABLE II

Conduction Parameters of Channels in Neutral and Charged Bilayers

	Channel conductance			
	PE	PS/PE, 50 mM	PS/PE, 500 mM	d
	pS			*Å*
SR K channel (Bell and Miller, 1984)	220	2.8	1.2	10
Ca-activated K channel (Moczydlowski et al., 1985)	404	2.2	1.1	9
Ca channel sodium current (present data)	68	1.8	1.0	20
Batrachotoxin-activated Na channel (Worley, J. F., B. K. Krueger, and R. J. French, personal communication)	31	1.2	1.1	>20

PE corresponds to the saturating channel conductance in pure PE bilayers; PS/PE corresponds to the conductance ratio in pure PE and pure PS at 50 or 500 mM ion concentration; d is the fitted insulation distance from the channel entryway to the plane of the lipid charges (Eqs. 5*a*, 5*b*, and 6).

lipid), but equally well as an horizontal distance (parallel to the plane of the lipid). In the vertical model, insulation from the lipid is given by the protrusion of the mouth of the channel out into bulk solution (Bell and Miller, 1984). In the horizontal model, insulation is given by the thickness of the channel wall, while the mouths of the channel are set at the bilayer surface (Apell et al., 1979). Obviously, a combination of these two limiting cases is also possible and is probably more realistic. Regardless of the final interpretation, it is clear that the distances given in Table II can only be physically realized by proteins of large dimensions. An already classic example is the acetylcholine receptor with M_r 280,000, extending ~55 Å into the synaptic space and 15 Å into the cytoplasmic space (Kistler et al., 1982). In such a massive structure, the ion entryways at the ends of the protein appear to be completely insensitive to electrostatic surface phenomena (Criado et al., 1984). Similar arguments can be raised for the sodium channel, a predominant polypeptide of M_r 260,000 (Weigele and Barchi, 1982), and for the nitrendipine-binding complex associated to the calcium channel (Ferry et al., 1983; Curtis and Catterall, 1984; Borsotto et al., 1984).

We are grateful to Drs. Jeffrey S. Smith and Sidney Simon for comments and suggestions at various stages of this project.
This work was supported by National Institutes of Health grant RO1 GM-32824.

Original version received 10 October 1985 and accepted version received 11 February 1986.

REFERENCES

Affolter, H., and R. Coronado. 1985*a*. Planar bilayer recording of single calcium channels from purified muscle transverse tubules. *Biophysical Journal.* 47:434*a*. (Abstr.)

Affolter, H., and R. Coronado. 1985*b*. Agonists Bay-K8644 and CGP-28392 open calcium channels reconstituted from skeletal muscle transverse tubules. *Biophysical Journal.* 48:341–347.

Affolter, H., and R. Coronado. 1985*c*. The sidedness of reconstituted calcium channels from muscle transverse tubules as determined by D600 and D890 blockade. *Biophysical Journal.* 49:767–771.

Akaike, N., K. Lee, and A. M. Brown. 1978. The calcium current of *Helix* neuron. *Journal of General Physiology.* 71:509–531.

Almers, W., and E. W. McCleskey. 1984. Non-selective conductance in calcium channels of frog muscle: calcium selectivity in a single-file pore. *Journal of Physiology.* 353:585–608.

Apell, H. J., E. Bamberg, and P. Lauger. 1979. Effect of surface charge on the conductance of the gramicidin channel. *Biochimica et Biophysica Acta.* 522:369–378.

Begenisich, T. 1975. Magnitude and location of surface charges on *Myxicola* giant axons. *Journal of General Physiology.* 66:47–65.

Bell, J., and C. Miller. 1984. Effects of phospholipid surface charge on ion conduction in the K^+ channel of sarcoplasmic reticulum. *Biophysical Journal.* 45:279–287.

Borsotto, M., R. I. Norman, M. Fosset, and M. Lazdunski. 1984. Solubilization of the nitrendipine receptor of skeletal muscle transverse tubule membranes: interactions with specific inhibitors of the voltage-dependent calcium channel. *European Journal of Biochemistry.* 142:449–455.

Butler, J. N. 1968. The thermodynamic activity of calcium ion in sodium chloride-calcium chloride electrolytes. *Biophysical Journal.* 8:1426–1433.

Byerly, L., P. B. Chase, and J. R. Stimers. 1985. Permeation and interaction of divalent cations in calcium channels of snail neurons. *Journal of General Physiology.* 85:491–518.

Carnie, S., and S. McLaughlin. 1983. Large divalent cations and electrostatic potential adjacent to membranes. A theoretical calculation. *Biophysical Journal.* 44:325–332.

Colquhoun, D., and F. J. Sigworth. 1983. Fitting and statistical analysis of single channel records. *In* Single Channel Recording. B. Sakmann and E. Neher, editors. Plenum Press, New York. 191–263.

Coronado, R., and H. Affolter. 1985*a*. Kinetics of dihydropyridine-sensitive single calcium channels from purified muscle transverse tubules. *Biophysical Journal.* 47:434*a*. (Abstr.)

Coronado, R., and H. Affolter. 1985*b*. Characterization of dihydropyridine-sensitive calcium channels from purified skeletal muscle transverse tubules. *In* Ion Channel Reconstitution. C. Miller, editor. Plenum Press, New York. In press.

Coronado, R., R. Rosenberg, and C. Miller. 1980. Ionic selectivity saturation and block in a K^+-selective channel from sarcoplasmic reticulum. *Journal of General Physiology.* 76:425–446.

Cota, G., and E. Stefani. 1984. Saturation of calcium channels and surface charge effects in skeletal muscle fibres of the frog. *Journal of Physiology.* 351:135–154.

Criado, M., H. Eibl, and F. J. Barrantes. 1984. Functional properties of the acetylcholine receptor incorporated in model membranes. Differential effects of chain length and head group of phospholipids on receptor affinity states and receptor-mediated ion translocation. *Journal of Biological Chemistry.* 259:9188–9198.

Curtis, B. M., and W. A. Catterall. 1984. Purification of the calcium antagonist receptor of the voltage-sensitive calcium channel from skeletal muscle transverse tubules. *Biochemistry.* 23:2113–2117.

Ferry, D. R., A. Goll, and H. Glossmann. 1983. Differential labelling of putative skeletal muscle calcium channels by [^{3}H]nifedipine, [^{3}H]nitrendipine, [^{3}H]nimodipine, and [^{3}H]-PN 200-110. *Naunyn-Schmiedeberg's Archiv für Pharmakologie.* 323:276–277.

Fohlmeister, J. F., and W. J. Adelman. 1982. Periaxonal surface calcium binding and distribution of charge on the faces of the squid axon potassium channel molecules. *Journal of Membrane Biology.* 70:115–123.

Frankenhaeuser, B., and A. L. Hodgkin. 1957. The action of calcium on the electrical properties on the squid axon. *Journal of Physiology.* 137:218–244.

Gilbert, D. L., and G. Ehrenstein. 1969. Effect of divalent cations on potassium conductance of squid axons. *Biophysical Journal.* 9:447–463.

Hagiwara, S. 1975. Ca-dependent action potential. *In* Membranes: A Series of Advances. 3rd edition. G. Eisenman, editor. Marcel Dekker, New York. 359–382.

Hahin, D. T., and D. T. Campbell. 1983. Simple shifts in the voltage dependence of sodium channel gating caused by divalent cations. *Journal of General Physiology.* 82:785–805.

Harned, H. S., and B. B. Owen. 1950. The physical chemistry of electrolytic solutions. American Chemical Society Monograph Series. Reinhold Publishing Corp., New York. 412.

Hess, P., and Tsien, R. W. 1984. Mechanism of ion permeation through calcium channels. *Nature.* 309:453–456.

Hille, B., A. M. Woodhull, and T. Shapiro. 1975. Negative surface charge near sodium channels of nerve: divalent ions, monovalent ions, and pH. *Philosophical Transactions of the Royal Society of London B Biological Sciences.* 270:301–318.

Kistler, J. R., M. Stroud, Klykowsky, R. A. Lalancette, and R. H. Fairclough. 1982. Structure and function of an acetylcholine receptor. *Biophysical Journal.* 37:371–383.

Kostyuk, P. G., O. A. Krishtal, and P. A. Doroshenko. 1974. Calcium currents in snail neurons. *Pflügers Archiv European Journal of Physiology.* 348:95–104.

Kostyuk, P. G., S. L. Mironov, P. A. Doroshenko, and V. N. Ponomarev. 1982. Surface charge on the outer side of mollusc neuron membrane. *Journal of Membrane Biology.* 70:171–179.

Kostyuk, P. G., S. L. Mironov, and Y. M. Shuba. 1983. Two ion-selecting filters in the calcium channel of the somatic membrane of mollusc neurons. *Journal of Membrane Biology.* 76:83–93.

Loosley-Millman, M. E., R. P. Rand, and V. A. Parsegian. 1982. Effect of monovalent ion binding and screening and measured electrostatic forces between charged phospholipid bilayers. *Biophysical Journal.* 40:221–232.

McCleskey, E. W., and W. Almers. 1985. The Ca channel in skeletal muscle is a large pore. *Proceedings of the National Academy of Sciences.* 82:7149–7153.

McCleskey, E. W., P. Hess, and R. W. Tsien. 1985. Interaction of organic cations with the calcium channel. *Journal of General Physiology.* 86:22*a*. (Abstr.)

McLaughlin, S., G. A. N. Mulrine, T. Gresalfi, G. Vaio, and A. McLaughlin. 1981. Adsorption of divalent cations to bilayer membranes containing phosphatidylserine. *Journal of General Physiology.* 77:445–473.

McLaughlin, S. G. A., G. Szabo, and G. Eisenman. 1971. Divalent ions and the surface potential of charged phospholipid membranes *Journal of General Physiology.* 58:667–687.

Moczydlowski, E., O. Alvarez, C. Vergara, and R. Latorre. 1985. Effect of phospholipid charge on the conductance and gating of a Ca^{2+}-activated K^+ channel in planar bilayers. *Journal of Membrane Biology.* 83:273–282.

Mozhayeva, G. N., and H. P. Naumov. 1970. Effect of surface charge on the steady-state potassium conductance of nodal membrane. *Nature.* 228:164–165.

Ohmori, H., and M. Yoshii. 1977. Surface potential reflected in both gating and permeation mechanisms of sodium and calcium channel of the tunicate egg cell membrane. *Journal of Physiology.* 267:429–463.

Rosemblatt, M., C. Hidalgo, C. Vergara, and I. Ikemoto. 1981. Immunological and biochemical properties of transverse tubule membranes isolated from rabbit skeletal muscle. *Journal of Biological Chemistry.* 256:8140–8148.

Weigele, D. J., and R. Barchi. 1982. Functional reconstitution of the sodium channel from rat sarcolemma. *Proceedings of the National Academy of Sciences.* 79:3653–3655.

Wilson, D. L., K. Morimoto, Y. Tsuda, and A. M. Brown. 1983. Interaction between calcium ions and surface charge as it relates to calcium currents. *Journal of Membrane Biology.* 72:117–130.